Clinical Radiology 74 (2019) 325.e19–325.e24

Contents lists available at ScienceDirect

Clinical Radiology

journal homepage: www.clinicalradiologyonline.net

Differentiation malignant from benign pericardial effusion with diffusion-weighted MRI

A.A.K.A. Razek*, S. Samir

Department of Diagnostic Radiology, Mansoura Faculty of Medicine, Masnoura, Egypt

ARTICLE INFORMATION

Article history:
Received 26 June 2018
Accepted 8 January 2019

AIM: To differentiate malignant from benign pericardial effusion with diffusion-weighted magnetic resonance imaging (MRI).

MATERIAL AND METHODS: Retrospective analysis of diffusion-weighted MRI of 41 patients (29 men and 12 women; mean 39 years) with pericardial effusion. Apparent diffusion coefficient (ADC) of pericardial fluid, and associated pericardial mass or pleural effusion was calculated. ADC of pericardial fluid was calculated by two observers and correlated with cytological analysis. Receiver operating characteristic curves and Bland–Altman plots were used.

RESULTS: There was significant differences in the ADCs between benign and malignant pericardial effusions (p=0.001) by both observers. Mean ADC of malignant pericardial effusions was (2.92±0.29 and 2.86±0.33×10^{-3} mm^2/s) and of benign effusions was (3.36±0.31 and 3.28±0.28×10^{-3} mm^2/s) for both observers, respectively. The cut-off values of the ADC used for differentiating malignant from benign pericardial effusion were 3.25 and 3.05×10^{-3} mm^2/s with areas under curve of 0.839 and 0.791, sensitivities of 88.2% and 70.6%, specificities of 69.6% and 73.9%, and accuracies of 78% and 72.5% for both observers, respectively. The overall interobserver agreement of the ADC value of pericardial effusion by both observers was significant (r=0.808, p=0.001). The interobserver agreement of malignant effusion (r=0.861, p=0.001) and benign effusion was significant (r=0.659, p=0.001). The ADC of pleural effusion is well correlated with ADC of pericardial effusion (r=0.088, p=0.001).

CONCLUSION: The ADC value is a non-invasive imaging parameter that can be used for differentiation of malignant from benign pericardial fluid.

Introduction

Pericardial effusion is a relatively common finding in a clinical practice that may be associated with several malignant tumours and benign lesions. Determining the nature of pericardial effusion either malignant or benign is often critical in patient management.[1–5] Echocardiography is the initial imaging method for diagnosis of pericardial effusion, but it cannot differentiate malignant from benign effusion and it is operator dependent.[6,7] Computed tomography (CT) can detect the presence of pericardial effusion, but it is associated with radiation exposure.[8,9] Routine pulse sequences of magnetic resonance imaging (MRI) as balanced steady-state free precession sequences and double or triple inversion recovery fast spin-echo sequences can detect pericardial effusions, but it cannot accurately characterise their nature.[10–12] Paracentesis is the definite diagnosis, but may be associated with haemorrhage and it is an invasive procedure.[1,13]

* Guarantor and correspondent: A. A. K. A. Razek, Department of Diagnostic Radiology, Mansoura Faculty of Medicine, Masnoura, Egypt. Tel.: +201061948567.

E-mail address: arazek@mans.edu.eg (A.A.K.A. Razek).

https://doi.org/10.1016/j.crad.2019.01.005
0009-9260/

Diffusion-weighted MRI can provide better characterisation of fluid because it reflects the random motion of water protons, which is disturbed by intracellular organelles and macromolecules located in the tissues. Thus, the ADC values of the tissues vary according to the nature and content of the fluid.[14–16] Recently, diffusion-weighted MRI was used in the chest for evaluation of mediastinal masses and bronchogenic tumours.[15–17] Only, one study discussed the role of diffusion-weighted MRI in pleural effusion.[18] To the authors' knowledge, there is no previous study in the English literature that has discussed the apparent diffusion coefficient (ADC) of pericardial effusion. Therefore, the aim of the present study was to differentiate malignant from benign pericardial effusion using diffusion-weighted MRI.

Material and methods

Patients

This study was approved by institutional ethics committee and informed consent was waived because this was a retrospective study. This retrospective study was performed, during the period between November 2006 and November 2016. The study included 44 patients with pericardial effusions. The inclusion criteria were patients with pericardial effusion at MRI who underwent diffusion-weighted MRI. The patients were referred for MRI for staging of chest or breast malignancy, suspected pericardial tumours or to search for the cause of pericardial effusion. Three patients were excluded from the study due to poor image quality with susceptibility artefacts. The final patients included in this study were 41 patients with pericardial effusion. The final diagnosis was based upon cytological examination of pericardial effusion from pericardiocentesis (n=28) and histopathological examination of pericardial mass from biopsy (n=13).

Routine MRI

MRI was performed using a 1.5 T MRI system (symphony; Siemens Medical systems, Erlangen, Germany) with application of automatic multi-angle-projection shim and the chemical shift selective fat-suppression (CHESS) technique to reduce artefacts of MRI. The motion-probing gradient was applied before and after the 180 pulse with echo-planar imaging readout. All patients underwent axial and coronal true fast imaging employing steady state precession (FISP; using a repetition time [TR] of 4.3 ms and echo time [TE] of 2.1 ms) with a section thickness of 5 mm, an intersection gap of 1–2 mm, a field of view (FOV) of 25–35 cm, and an acquisition matrix of 256×256.

Diffusion MRI

Diffusion-weighted MRI images were obtained using a multi-slice spin-echo single shot echo-planar imaging sequence. Imaging parameters were 10,000 ms TR, 108 ms TE, 20×23 cm field of view (FOV), an acquisition matrix of 256×128, and section thickness of 5 mm with an inter-slice gap of 1–2 mm. Diffusion probing gradients were applied in the three orthogonal directions (x, y, and z). Diffusion-weighted MRI images were acquired with diffusion-weighted factor, factor b of 0, 500, and 1,000 s/mm^2. The data acquisition time for the diffusion-weighted images was 2 minutes. The ADC maps were reconstructed using commercial workstation with standard software (Leonardo console software, version 2.0; Siemens AG Medical Solutions, Forchheim, Germany).

Image analysis

A quantitative analysis of the apparent diffusion coefficient map was made. The ADC values were calculated by two radiologists with experience of 22 and 12 years in MRI, respectively. They independently calculated the ADC values blinded to the patient data and the final diagnosis. A region of interest was placed in the pericardial effusion by each radiologist using the electronic cursor in three regions of the pericardial fluid (Fig 1). The region of interest was selected to be away from the regions of artefact. Each radiologist took the mean of these three values, and calculated and represented the final ADC value per patient that was used for statistical analysis. Another region of interest was placed in the solid part of the associated pericardial malignant tumour in 13 patients and associated pleural effusion in 18 patients.

Statistical analysis

The description of data was done in the form of means and standard deviations (SDs). Student's t-test was used to detect significant differences in the ADC values of malignant and benign pericardial and pleural effusions. A p-value of $\leq$0.05 was considered significant if at 95% confidence interval. Bland–Altman plots were used for agreement of ADC value between both observers. Receiver operating curve (ROC) characteristics were calculated to determine the cut-off point that was used to differentiate malignant from benign pericardial effusion with calculation of area under the curve, accuracy, sensitivity, specificity, and positive predictive and negative predictive values. The statistical analysis of the data was done by using the SPSS program (Statistical Package for Social Science version 20).

Results

Patients with pericardial effusion were 29 men and 12 women aged 22–68 years, mean 39 years. The patients were presented with dyspnoea (n=37), and chest pain (n=34). The causes of pericardial effusion were malignant (n=17) and benign (n=24). The causes of malignant (Fig 1) pericardial effusions were non-small cell lung cancer (n=5), lymphoma (n=4), breast cancer (n=4), malignant thymoma (n=2), and pleural mesothelioma (n=2). The causes of benign (Fig 2) pericardial effusions were congestive heart failure (n=5), systemic lupus erythromatosus (n=4), anti-phospholipid antibody syndrome (n=3), chronic renal failure (n=3), tuberculosis (n=3), and unknown (n=6).

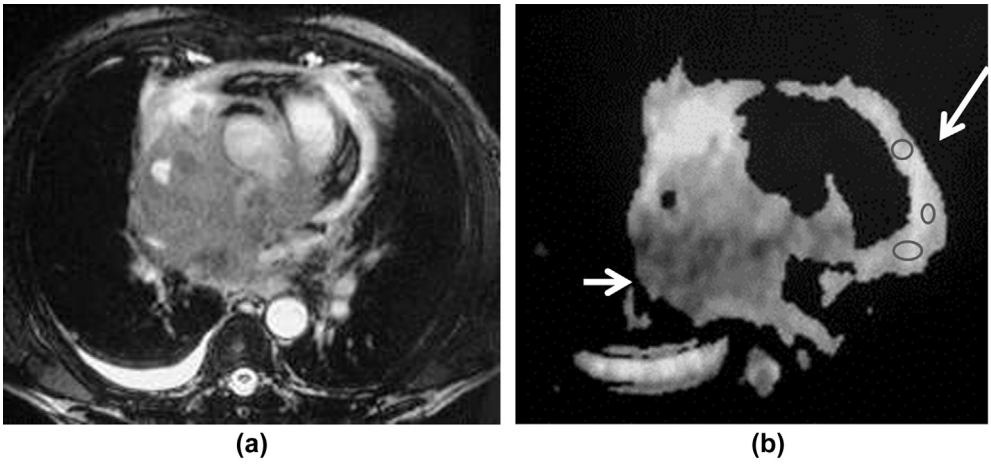

Figure 1 Malignant pericardial effusion. (a) Axial true-FISP MRI image shows hyper-intense pericardial effusion in a patient with malignant thymoma. (b) ADC map shows localisation of three regions of interest within the pericardial effusion (long arrow) with a calculated ADC value of 2.92×10^{-3} mm^2/s. The malignant thymoma (short arrow) shows unrestricted diffusion with a low ADC value (0.99×10^{-3} mm^2/s).

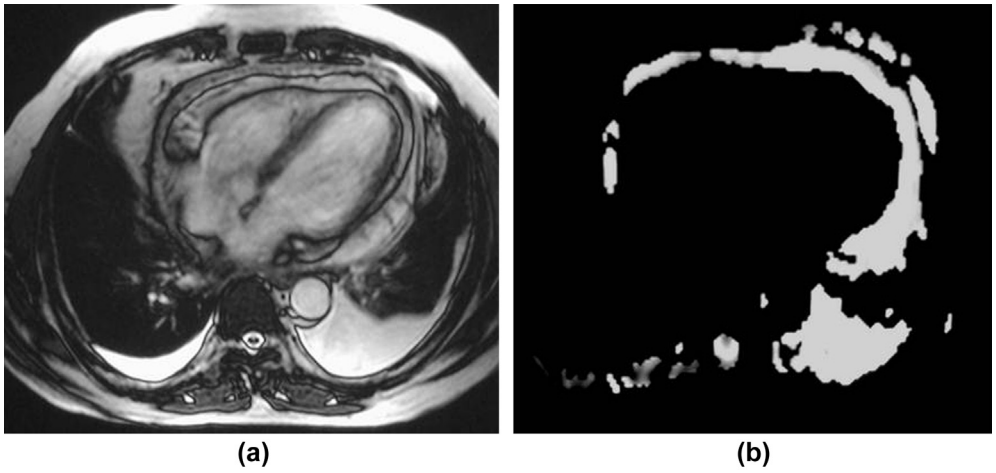

Figure 2 Benign pericardial effusion. (a) Axial true-FISP MRI image shows hyper-intense pericardial effusion in a patient with benign pericardial effusion. (b) ADC map showing unrestricted diffusion of pericardial effusion. The mean ADC value of pericardial effusion was 3.12×10^{-3} mm^2/s.

There was a statistically significant difference (p=0.001) in the ADC values between benign and malignant pericardial effusions of both observers. The mean ADC values of malignant pericardial effusions were 2.92±0.29 and $2.86\pm0.33\times10^{-3}$ mm^2/s and benign pericardial effusions were 3.36±0.31 and $3.28\pm0.28\times10^{-3}$ mm^2/s for both observers, respectively (Fig 3). The cut-off values of ADC value used to differentiate malignant from benign pericardial effusion were 3.25 and 3.05×10^{-3} mm^2/s with areas under the curve of 0.839 and 0.791, sensitivities of 88.2% and 70.6%, specificities of 69.6% and 73.9%, accuracies of 78% and 72.5%, negative predictive values of 89.5% and 77.3%, and positive predictive values of 68.2% and 66.7% for both observers, respectively (Fig 4; Table 1). The overall interobserver agreement of the ADC value of pericardial effusions by both observers was significant (r=0.808, p=0.001; Fig 5). The interobserver agreement of malignant effusion (r=0.861, p=0.001) and benign effusion (r=0.659, p=0.001) was significant.

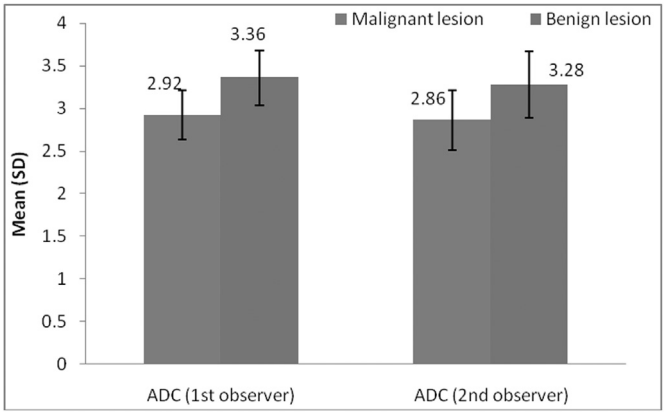

Figure 3 Box plot of the ADC value of pericardial effusion obtained by the two observers. The mean ADC values of malignant pericardial effusions were 2.92±0.29 and $2.86\pm0.33\times10^{-3}$ mm^2/s and benign pericardial effusions were 3.36±0.31 and $3.28\pm0.28\times10^{-3}$ mm^2/s for both observers, respectively.

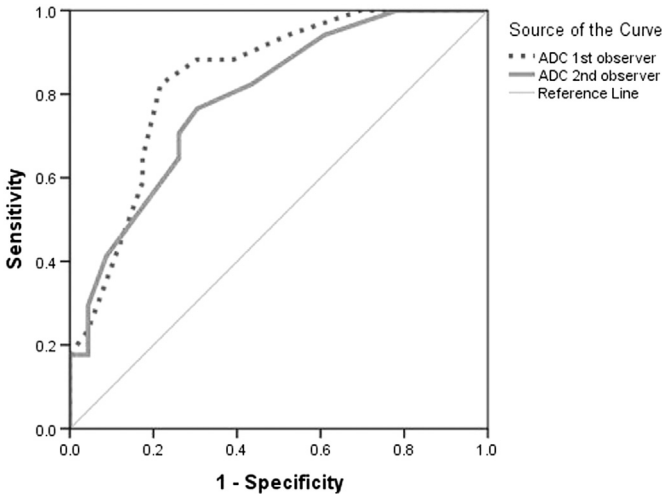

Figure 4 ROC curves obtained by both observers. The cut-off values of the ADC value used for differentiation of malignant from benign pericardial effusion were 3.25 and 3.05×10^{-3} mm^2/s with areas under curve of 0.839 and 0.791, sensitivities of 88.2% and 70.6%, specificities of 69.6% and 73.9%, and accuracies of 78% and 72.5% for both observers, respectively.

There was misdiagnosis in three patients. Two patients with malignant pericardial effusion exhibited high ADC, and were misdiagnosed as having benign effusion while another patient with benign pericardial effusion exhibited low ADC and was misdiagnosed as having malignant effusion.

Malignant pericardial effusion was associated with pericardial mass in 13 patients. The ADC of pericardial metastasis from non-small cell lung cancer (n=5) was 1.09 ± 0.19 $(0.9–1.31)\times10^{-3}$ mm^2/s, lymphomas (n=4) was 0.77 ± 0.03 $(0.74–0.82)\times10^{-3}$ mm^2/s, malignant thymoma (n=2) was 0.89 ± 0.13 $(0.80–0.99)\times10^{-3}$ mm^2/s, and pleural mesotheliomas (n=2) was 1.15 ± 0.18 $(1.02–1.27)\times10^{-3}$ mm^2/s. There was no significant difference (p=0.70 and 0.60) in the ADC values of different malignant pericardial masses by both observers, but malignant lymphomas showed lowest ADC values within malignant pericardial masses. There was no significant correlation between ADC of the pericardial mass and effusion (r=0.801, p=0.51).

Pericardial effusion was associated with pleural effusion in 18 patients. The mean ADC value of malignant pleural effusion (n=11) was $(2.83\pm0.29\times10^{-3}$ $mm^2/s)$ was significantly different (p=0.001) than that of benign effusion (n=7) was $3.25\pm0.31\times10^{-3}$ mm^2/s. There was positive correlation between the ADC value of pericardial and associated pleural effusion (r=0.088, p=0.001).

Discussion

The main findings in this work are the presence of a significant difference in ADC value of malignant and benign pericardial effusion and correlation of the ADC value of pericardial effusion with the ADC value of pleural effusion.

In the present study, the mean ADC value of malignant pericardial effusion was significantly lower (p=0.001) than that of benign pericardial effusion. This may be attributed to difference in the biological structures, such as cellular structures and protein binding, as well as physical parameters such as high viscosity of the malignant and benign pericardial fluid. Malignant effusion is an exudative fluid that is composed of high protein and cell counts, and may show fibrous strands as well as haemorrhagic fluid that decreases the viscosity of the fluid with restricted diffusion.[1–5] In addition, the presence of malignant cells within the fluid increases cellularity with subsequent restricted diffusion and lower ADC value. Benign pericardial effusion is composed of exudative fluid with less protein and cell counts represented by increased ADC values.[8]

In the present study, there is overlap between the ADC values of malignant and benign pericardial effusions. Patients with tuberculous pericardial effusion exhibiting restricted diffusion with low ADC value were misdiagnosed as malignant effusion. This is attributed to the presence of excess fibrous tissue within the pericardial fluid with subsequent restriction of diffusion.[19] In addition, malignant pericardial effusion may reveal high ADC values due to presence of few malignant cells within the pericardial effusion.[14]

Previous studies have reported that the ADC value of mediastinal lymphomas was lower than that of metastatic lesions[20,21] and diffusion-weighted MRI may be helpful in the characterisation of mediastinal masses, thymic tumours, and bronchogenic carcinomas.[20–22] In this study, associated pericardial malignant lymphoma shows lower ADC values than other pericardial malignant tumours. This may be attributed to higher cellularity of malignant lymphomas compared to other malignancy; however, there was no significant difference in ADC values of different pericardial malignant masses. Further studies on large numbers of patients with pericardial mass will better characterise pericardial tumours in the future.

In the present study, there was a significant difference in the ADC values of malignant pleural effusion than benign effusion and the ADC value of pleural effusion correlated with the ADC value of pericardial effusion. Previous studies have reported that there is a significant difference in the

Table 1
Receiver operating characteristic (ROC) curve results with calculation of sensitivity and specificity of both observers.

ADC	AUC (95%CI) p-value	Cut-off points	Sensitivity %	Specificity %	Accuracy %	NPV %	PPV %
Observer 1	0.839 (0.71–0.96) p=0.001	≤3.25	88.2	69.6	78	89.5	68.2
Observer 2	0.791 (0.65–0.93) p=0.002	≤3.05	70.6	73.9	72.5	77.3	66.7

ADC, apparent diffusion coefficient; AUC, area under the ROC curve; NPV, negative predictive value; PPV, positive predictive value.

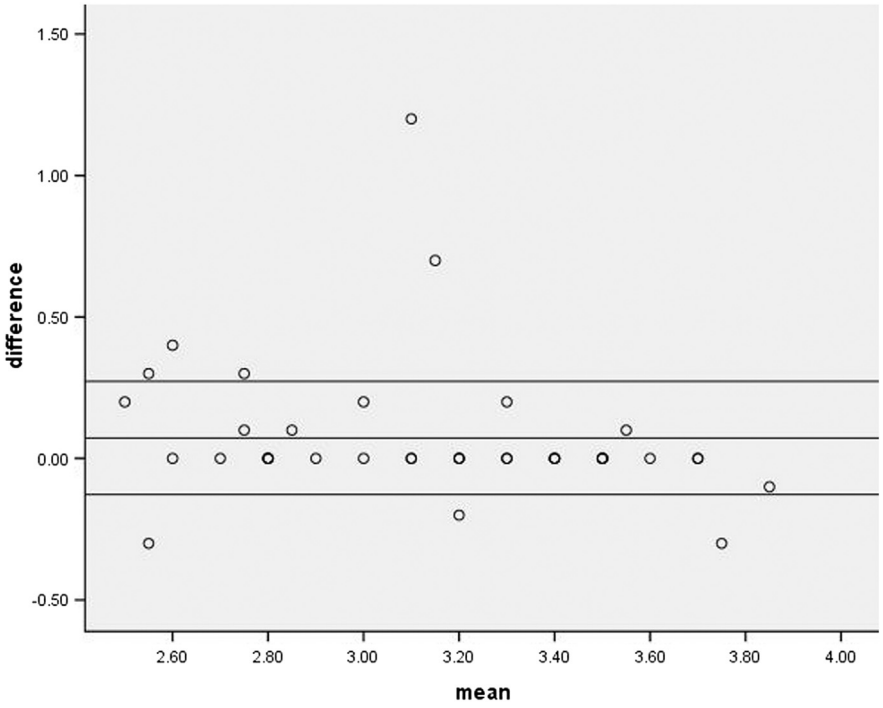

Figure 5 Bland–Altman plots for agreement of ADC values of pericardial effusions by both observers (r=0.808, p=0.001).

ADC value between exudative and transudative pleural effusion.[18]

There are some limitations of this study. First, this study is retrospective with potential selection bias of patients and a small number of patients. Further prospective studies comprising large numbers of patients with pericardial effusion and pericardial masses will improve the results. Second, this study applied echo-planar diffusion-weighted MRI at 1.5 T. Further studies with the application of diffusion tensor MRI,[23–26] arterial spin labelling[27,28] with advanced post-processing methods and machine learning using higher magnet strengths may provide a better characterisation of pericardial effusion.[29–33] Third, the difference in parameters of pulse sequences and scanner could affect the ADC values of pericardial effusion. Standardisation and updating of parameters of pulse sequences of different scanners improves the analysis of different studies.

In conclusion, ADC values can be used to differentiate malignant from benign pericardial effusion.

Conflict of interest

The authors declare no conflict of interest.

References

1. Vakamudi S, Ho N, Cremer PC. Pericardial effusions: causes, diagnosis, and management. *Prog Cardiovasc Dis* 2017;**59**:380–8.
2. Cummings KW, Green D, Johnson WR, *et al*. Imaging of pericardial diseases. *Semin Ultrasound CT MR* 2016;**37**:238–54.
3. Cremer PC, Kwon DH. Multimodality imaging of pericardial disease. *Curr Cardiol Rep* 2015;**17**:24.
4. Czum JM, Silas AM, Althoen MC. Evaluation of the pericardium with CT and MR. *ISRN Cardiol* 2014;**2014**:174908.
5. Bogaert J, Francone M. Pericardial disease: value of CT and MRI. *Radiology* 2013;**267**:340–56.
6. Alter P, Figiel JH, Rupp TP, *et al*. MR, CT, and PET imaging in pericardial disease. *Heart Fail Rev* 2013;**18**:289–306.
7. Dawson D, Rubens M, Mohiaddin R. Contemporary imaging of the pericardium. *J Am Coll Cardiol Img* 2011;**4**:680–4.
8. Rajiah P, Kanne JP. Computed tomography of the pericardium and pericardial disease. *J Cardiovasc Comput Tomogr* 2010;**4**:3–18.
9. Sun J, Park K, Kang D. CT Findings in patients with pericardial effusion: differentiation of malignant and benign disease. *AJR Am J Roentgenol* 2010;**194**:W489–94.
10. Young PM, Glockner JF, Williamson EE, *et al*. MRI findings in 76 consecutive surgically proven cases of pericardial disease with CT and pathologic correlation. *Int J Cardiovasc Imag* 2012;**28**:1099–109.
11. Bogaert J, Francone M. Cardiovascular magnetic resonance in pericardial diseases. *J Cardiovasc Magn Reson* 2009;**11**:14.
12. Misselt AJ, Harris SR, Glockner J, *et al*. MRI of the pericardium. *Magn Reson Imag Clin N Am* 2008;**16**:185–99.
13. Saab J, Hoda RS, Narula N, *et al*. Diagnostic yield of cytopathology in evaluating pericardial effusions: clinicopathologic analysis of 419 specimens. *Cancer* 2017;**125**:128–37.
14. Razek AA. Diffusion magnetic resonance imaging of chest tumors. *Cancer Imag* 2012;**12**:452–63.
15. Razek AA, Elmorsy A, Elshafey M, *et al*. Assessment of mediastinal tumors with diffusion-weighted single-shot echo-planar MRI. *J Magn Reson Imag* 2009;**30**:535–40.
16. Razek AA, Fathy A, Gawad TA. Correlation of apparent diffusion coefficient value with prognostic parameters of lung cancer. *J Comput Assist Tomogr* 2011;**35**:248–52.
17. Abdel Razek AA, Soliman N, Elashery R. Apparent diffusion coefficient values of mediastinal masses in children. *Eur J Radiol* 2012;**81**:1311–4.
18. Baysal T, Bulut T, Gökirmak M, *et al*. Diffusion-weighted MRI of pleural fluid: differentiation of transudative vs exudative pleural effusions. *Eur Radiol* 2004;**14**:890–6.
19. Cherian G, Uthaman B, Salama A, *et al*. Tuberculous pericardial effusion: features, tamponade, and computed tomography. *Angiology* 2004;**55**:431–40.
20. Abdel Razek AA, Gaballa G, Elashry R, *et al*. Diffusion-weighted MRI of mediastinal lymphadenopathy in children. *Jpn J Radiol* 2015;**33**:449–54.

21. Abdel Razek AA, Elkammary S, Elmorsy AS, *et al*. Characterisation of mediastinal lymphadenopathy with diffusion-weighted imaging. *Magn Reson Imag* 2011;**29**:167–72.
22. Abdel Razek AA, Khairy M, Nada N. Diffusion-weighted MR imaging in thymic epithelial tumors: correlation with World Health Organization classification and clinical staging. *Radiology* 2014;**273**:268–75.
23. Razek AAKA. Diffusion tensor imaging in differentiation of residual head and neck squamous cell carcinoma from post-radiation changes. *Magn Reson Imag* 2018;**54**:84–9.
24. Mekkaoui C, Reese TG, Jackowski MP, *et al*. Diffusion MRI in the heart. *NMR Biomed* 2017;**30**:e3426.
25. Khalek Abdel Razek AA. Characterization of salivary gland tumours with diffusion tensor imaging. *Dentomaxillofac Radiol* 2018;**47**:20170343.
26. MacGowan GA, Parikh JD, Hollingsworth KG. Diffusion tensor magnetic resonance imaging of the heart: looking into the layers of the myocardium. *J Am Coll Cardiol* 2017;**69**:677–8.
27. Abdel Razek AAK, Nada N. Arterial spin labeling perfusion-weighted MRI: correlation of tumor blood flow with pathological degree of tumor differentiation, clinical stage and nodal metastasis of head and neck squamous cell carcinoma. *Eur Arch Otorhinolaryngol* 2018;**275**:1301–7.
28. Abdel Razek AAK. Arterial spin labelling and diffusion-weighted magnetic resonance imaging in differentiation of recurrent head and neck cancer from post-radiation changes. *J Laryngol Otol* 2018;**132**:923–8.
29. Abdel Razek A, Mossad A, Ghonim M. Role of diffusion-weighted MRI in assessing malignant versus benign skull-base lesions. *Radiol Med* 2011;**116**:125–32.
30. Abdel Razek AA, Elkhamary S, Al-Mesfer S, *et al*. Correlation of apparent diffusion coefficient at 3T with prognostic parameters of retinoblastoma. *AJNR Am J Neuroradiol* 2012;**33**:944–8.
31. Abdel Razek AA, Kamal E. Nasopharyngeal carcinoma: correlation of apparent diffusion coefficient value with prognostic parameters. *Radiol Med* 2013;**118**:534–9.
32. Razek AA, Gaballa G, Megahed AS, *et al*. Time resolved imaging of contrast kinetics (TRICKS) MR angiography of arteriovenous malformations of head and neck. *Eur J Radiol* 2013;**82**:1885–91.
33. Abdel Razek AAK. Routine and advanced diffusion imaging modules of the salivary glands. *Neuroimaging Clin N Am* 2018;**28**:245–54.